Journal of Biomechanics 129 (2021) 110849

Contents lists available at ScienceDirect

Journal of Biomechanics

journal homepage: www.elsevier.com/locate/jbiomech

Real-time kinematic-based detection of foot-strike during walking

Chrysostomos Karakasis, Panagiotis Artemiadis *

Department of Mechanical Engineering, University of Delaware, Newark, USA

ARTICLE INFO

Keywords:
Foot-strike
Real-time
Algorithm
Kinematics
Treadmill walking

ABSTRACT

Detection of foot-strike events is an integral part of gait analysis, as it allows the temporal registration of gait cycles. At the same time, it is necessary to register gait phases in real-time for applications such as wearable assistive devices and gait biofeedback that work synchronously with the human gait. Although many algorithms have been proposed for detecting foot-strikes with either wearable (e.g. Inertial Measurement Units (IMUs)) or non-wearable (e.g. force plates) sensors, there is a great need for real-time algorithms that rely only on recording the kinematics of the leg motion. This work proposes a novel and efficient kinematic algorithm, called the Foot VErtical & Sagittal Position Algorithm (F-VESPA), which has several advantages over existing methods. First, it accurately estimates foot-strike events using kinematic data without requiring access to future data points, hence achieving reduced latency during real-time implementation. Moreover, it does not require tuning of the utilized parameters, rendering it robust to different subjects and treadmill speeds. The algorithm is tested in a large set of subjects across various treadmill speeds, and it is shown to outperform even offline implementations of existing prominent kinematic algorithms. Using a 150 Hz data collection system, the F-VESPA achieved a median of 33 ms for the total true errors in detecting foot-strike. The F-VESPA is a highly responsive kinematic algorithm that can detect foot-strike events in real-time, with high accuracy, robustness and reduced latency, enabling real-time temporal registration of gait cycles.

1. Introduction

Precise characterization of individual gait events is critical for any gait analysis study. Human gait is separated into gait cycles, defined as the intervals between consecutive foot-strikes of the same foot (Perry et al., 1992). Hence, foot-strike detection techniques are usually employed for the temporal registration of gait cycles, as well the time normalization of data across multiple gait cycles. Thus, datasets obtained from different trials or subjects can be analyzed and compared in a meaningful way (Maiwald et al., 2009; O'Connor et al., 2007).

Numerous techniques have been proposed for foot-strike detection during gait. In general, these techniques can be separated into two categories based on whether they utilize wearable or non-wearable sensors (Taborri et al., 2016). In fact, non-wearable sensors stand out as the most accurate option for gait analysis in indoor experiments. Typical examples include force platforms and opto-electronic systems, with the former representing the gold standard in gait partitioning (Taborri et al., 2016; Tao et al., 2012). However, force platforms are not always available or suitable for certain studies, while they usually require specialized equipment that might increase the complexity of the experimental procedure (Hreljac and Marshall, 2000; Mickelborough et al., 2000). On the other hand, opto-electronic systems utilize kinematic methods, which represent the most popular technology found in clinical laboratories, while being recognized as the gold standard for routine gait analysis (Taborri et al., 2016).

Kinematic-based algorithms utilize 3D-kinematic data of the lower limbs recorded using a camera motion capture system (Rueterbories et al., 2010). Several kinematic algorithms have been published for foot-strike estimation, such as the Hreljac–Stergiou Algorithm (HSA) (Hreljac and Stergiou, 2000), Hreljac–Marshall Algorithm (HMA) (Hreljac and Marshall, 2000), Foot Vertical Velocity (FVELV) (Schache et al., 2001; Fellin et al., 2010) and Velocity-Based Treadmill Algorithm (VBTA) (Zeni Jr. et al., 2008). After an extensive research we performed in the literature amongst publications reviewing and comparing kinematic algorithms across different conditions and subjects, the Foot-Contact Algorithm (FCA) (Maiwald et al., 2009), the Foot-Velocity Algorithm (FVA) (O'Connor et al., 2007) and the Foot Vertical Position (FPOSV) method (Alton et al., 1998; Fellin et al., 2010) stood out as prominent due to their increased reported accuracy (Leitch et al., 2011; Sinclair et al., 2011; Fellin et al., 2010; Maiwald et al., 2009; Desailly et al., 2009; O'Connor et al., 2007; Alvim et al., 2015). A summary of the analysis above is illustrated in Table 1. However, most, if not all, kinematic algorithms that have been proposed so far provided only offline estimates for the foot-strike events. Although some of them have

* Correspondence to: Department of Mechanical Engineering, University of Delaware, 130 Academy Street, 126 Spencer Lab, Newark, DE 19716, USA.
E-mail address: partem@udel.edu (P. Artemiadis).

https://doi.org/10.1016/j.jbiomech.2021.110849
Accepted 25 October 2021
Available online 8 November 2021

been deployed in real-time in previous works (Roeles et al., 2018; Barkan et al., 2014), to the best of our knowledge, kinematic algorithms have never been evaluated both in terms or accuracy and latency during real-time implementation.

This is of high importance, as certain applications require real-time detection of gait phases, such as real-time control for wearable assistive devices (Kang et al., 2021; Holgate et al., 2009; Walsh et al., 2006), Function Electrical Stimulation (FES) and gait biofeedback (Hanlon and Anderson, 2009; Drolet et al., 2020). In these cases, wearable sensors have also been employed, such as Inertial Measurement Units (IMUs), foot-switches, etc., which allow for real-time detection even in outdoor environments (Kang et al., 2021; Walsh et al., 2006; Lind et al., 2009; Kormushev et al., 2012; Lim et al., 2015; Saccares et al., 2018; Dollar and Herr, 2008; Kadoya et al., 2014). However, despite the unique portability they offer, wearable sensors present certain drawbacks, such as challenging placement and reduced reliability and durability (Rueterbories et al., 2010; Tao et al., 2012). Therefore, the question arises of whether a kinematic algorithm could be devised for real-time implementation that would maintain high accuracy and minimal latency, without being restricted by the limitations of wearable sensors.

In order to address this gap, this work proposes and evaluates a novel kinematic algorithm, called the Foot VErtical & Sagittal Position Algorithm (F-VESPA).[1] The algorithm exhibits unique properties that provide significant advantages over existing algorithms. First, the F-VESPA predicts foot-strike events with high precision without requiring access to future data points, hence achieving reduced latency during real-time implementation. Furthermore, unlike previous works, tuning of the utilized parameters is not required, rendering the F-VESPA robust to different subjects and treadmill speeds. A comparative analysis was conducted in a large set of subjects across various treadmill speeds, where F-VESPA was shown to outperform even offline implementations of existing prominent kinematic algorithms. In summary, the F-VESPA is a highly responsive kinematic algorithm that can detect foot-strike events in real-time, with high accuracy, robustness and reduced latency, enabling real-time temporal registration of gait cycles.

2. Methods

The main aspect of this work is to evaluate a new real-time algorithm for foot-strike detection during walking, by comparing it with offline implementations of prominent existing algorithms using real kinematic data. For evaluation and comparison, we first define the set of kinematic and kinetic data used throughout the paper in Section 2.1. Then, the implementation of existing algorithms is discussed in Sections 2.2 and 2.3 . To the best of our knowledge, all existing algorithms have been proposed only for offline implementation. Hence, specific considerations and changes need to be made in order for them to be fairly compared with our proposed method. Finally, Section 2.4 details the proposed algorithm.

2.1. Description of dataset

In this work, we utilize data from a publicly available dataset (Fukuchi et al., 2018a,b). Specifically, in the study by Fukuchi et al. a group of 42 healthy subjects participated, consisting of 24 young and 48 older adults, respectively. Both kinematic and kinetic data were recorded during treadmill walking at a wide range of gait speeds. Kinematic data were collected at 150 Hz via a camera based motion-capture system (12 cameras, Raptor-4; Motion Analysis Corporation, Santa Rosa, CA, USA), while a dual-belt instrumented treadmill (FIT; Bertec, Columbus, OH, USA) measured the ground-reaction force data at 300 Hz. Lower-extremity kinematics were recorded by tracking the position of 26 anatomical reflective markers.

The treadmill walking experiments for each subject included trials at eight different controlled speeds: 40%, 55%, 70%, 85%, 100%, 115%, 130%, and 145% of the self-selected speed. The range of the self-selected speeds across subjects was 0.89–1.54 m/s.

For the calculation of the ground truth timing of the foot-strike events in the data, the measured vertical GRF component was utilized, as this represents the gold standard in gait partitioning. After applying a 4th order zero-phase low-pass Butterworth filter (cut-off frequency of 20 Hz), the GRF data were down-sampled to a frequency of 150 Hz, to match the kinematic sampling frequency. It should be noted that a zero-phase filter was adopted to derive the actual timing of the foot-strike events. For the foot-strike detection, a threshold value of 30 N on a rising edge was employed for the vertical GRF, which is within the documented range (5–40 N) of the literature (Alvim et al., 2015; Mickelborough et al., 2000; Hreljac and Stergiou, 2000; Hreljac and Marshall, 2000; Maiwald et al., 2009; Zeni Jr. et al., 2008; Leitch et al., 2011; Sinclair et al., 2013; Fellin et al., 2010; Sinclair et al., 2011; Hanlon and Anderson, 2009; O'Connor et al., 2007; Desailly et al., 2009). Fig. 1 demonstrates an example of ground truth timing identification for foot-strike events using the GRF component.

2.2. Implementation of the modified FCA

As analyzed in the Introduction Section, the FCA is one of the most accurate kinematic algorithms proposed in the literature. For that reason, it was implemented to provide a reference for the validation of the proposed algorithm. The details of its implementation are included below.

Due to the nature of the algorithm (Maiwald et al., 2009), a real-time implementation is not feasible, and therefore we opted for a modified implementation that includes an offline version with real-time filtering conditions. In detail, the three-dimensional kinematic data were filtered via a 2^{nd} order, low-pass Butterworth filter (cut-off at 20 Hz), without removing any introduced delays from the filter. The FCA detects touchdown using the vertical position of two markers: the posterior midsole of the heel ($HEEL$) and the lateral midsole at MTH5 ($MTH5$). Initially, all prominent local extrema that have a specific fixed prominence and an optimal minimum separation were derived. In particular, for the local minima, the optimal minimum separation values were derived to maximize the accuracy of the algorithm in each trial. Naturally, this procedure requires the knowledge of the whole signal throughout each trial.

Next, each trial was divided into segments using the prominent local maxima, and for each one the following procedure was followed. Initially, the timing of the earliest event between the prominent local minima of the two signals is set as the approximate time of touch down (TD_{approx}), while the corresponding marker is selected as the target marker. Based on that, the TI time interval is defined as:

$$TI = [TD_{approx} - o_1, TD_{approx} + o_2], \tag{1}$$

where $o_1 = 6$ samples and $o_2 = 12$ samples. The assigned size of the time interval was decided based on the trials and values noted in (Maiwald et al., 2009). Finally, the time instance of touchdown (or foot-strike) is defined as the most prominent local maximum in the vertical acceleration of the target marker during the time interval TI. The above procedure is repeated for all segments until the end of the trial in question. Fig. 2 demonstrates an example of foot-strike identification using the FCA.

[1] A preliminary version of this work is included in (Karakasis and Artemiadis, 2021).

Table 1
Comparison of kinematic algorithms for foot-strike detection. Each column corresponds to the publication cited in the top row and each row corresponds to a different kinematic algorithm. For each column-publication, ○ indicate which algorithms were included for evaluation and ×indicate which algorithms were classified as the most accurate. Cells are left blank when an algorithm was not evaluated in the respective publication. Kinematic algorithm abbreviations are as follows: Foot Vertical Position (FPOSV) (Alton et al., 1998; Pappas et al., 2001; Fellin et al., 2010), Hreljac–Marshall Algorithm (HMA) (Hreljac and Marshall, 2000), Hreljac–Stergiou Algorithm (HSA) (Hreljac and Stergiou, 2000), Custom Algorithm #1 (CA1) (Dingwell et al., 2001), Foot Vertical Velocity (FVELV) (Schache et al., 2001; Fellin et al., 2010), Custom Algorithm #2 (CA2) (Mickelborough et al., 2000), Foot-Velocity Algorithm (FVA) (O'Connor et al., 2007), Coordinate-Based Treadmill Algorithm (CBTA) (Zeni Jr. et al., 2008), Velocity-Based Treadmill Algorithm (VBTA) (Zeni Jr. et al., 2008), High-Pass Algorithm (HPA) (Desailly et al., 2009), Foot-Contact Algorithm (FCA) (Maiwald et al., 2009), Custom Algorithm #3 (CA3) (Leitch et al., 2011), and Vertical Displacement Algorithm (VDA) (Alvim et al., 2015). $CA1$–$CA3$ correspond to custom algorithms that were not identified by a specific name when proposed.

	Leitch et al., 2011	Sinclair et al., 2011	Fellin et al., 2010	Maiwald et al., 2009	Desailly et al., 2009	Alvim et al., 2015
FPOSV		×	×			×
HMA	○			○	○	
HSA	×	○	○	○		
CA1		×	○			
FVELV		○	×			
CA2		○				
FVA	×	×		○	×	×
CBTA		○	○			
VBTA		○				○
HPA					×	
FCA				×		×
CA3	○					
VDA						○

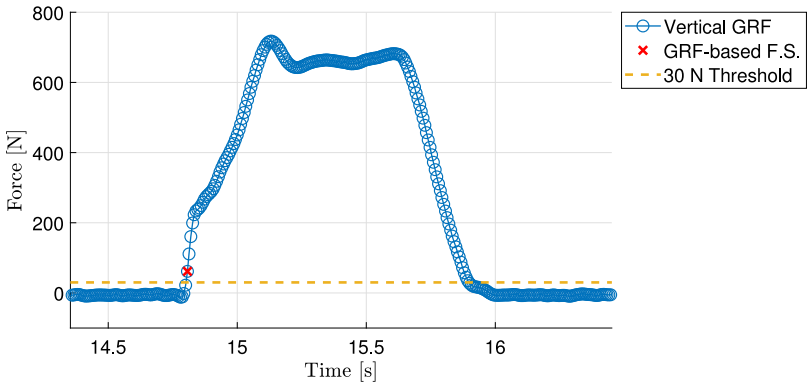

Fig. 1. Example of the ground truth timing identification using the GRF component. The chart shows the GRF component at a subject's left foot with respect to time. Circles (∘) indicate the samples of the measured vertical GRF component. Crosses (×) illustrate foot-strike events identified using a threshold on a rising edge. Dashed line represents the 30 N threshold applied. True foot-strikes are defined as the first samples that exceed the 30 N threshold on a rising edge.

2.3. Implementation of the modified FVA

Besides the FCA, another algorithm that stood out amongst the proposed algorithms in the literature is the FVA (O'Connor et al., 2007). Similarly to the FCA, a modified offline version was implemented for comparison purposes, as described below.

Since the metatarsal head II ($MTH2$) marker was not available in the employed dataset, the metatarsal head I ($MTH1$) marker was utilized instead, along with the $HEEL$ marker (O'Connor et al., 2007).

The same filtering with the FCA was applied to the kinematic data. Next, the midpoint between the vertical positions of the $HEEL$ and the $MTH1$ markers was computed, as a representation of the foot's center, while its vertical velocity was calculated via finite difference methods. Next, all prominent local minima in the vertical velocity of the foot's center were computed in each trial, by selecting the optimal minimum separation with respect to accuracy. Subsequently, in order to distinguish the specific local minima described in (O'Connor et al., 2007), constraints were imposed on the corresponding vertical position of the prominent local minima (max_{thld}, min_{thld}). The constraint imposed was that the foot center should be close to the ground level at foot-strike. Finally, the foot-strike events were defined as the frames that correspond to prominent negative local minima in the foot center's vertical velocity with a corresponding vertical position that satisfies the imposed thresholds. Fig. 3 demonstrates an example of foot-strike identification using the FVA.

2.4. Proposed Foot VErtical & Sagittal Position Algorithm (F-VESPA)

The proposed algorithm F-VESPA was designed in order to provide a robust and accurate method of detecting foot-strikes in real-time, using solely kinematic data. The algorithm can be considered as a significant extension of the FPOSV algorithm (Alton et al., 1998; Fellin et al., 2010), since instead of using only the vertical position, it also utilizes the sagittal position of the heel marker in the subject's leg. Throughout this paper, we will refer the position on the horizontal sagittal (antero-posterior) axis as the sagittal position. The motivation behind this was the fact that as the leg moves backwards, the rate of change in the sagittal position has a fixed sign[2]. As a consequence, this

[2] On the used dataset, the rate of change of the sagittal position was negative, but generally, it depends on each dataset formulation of the reference

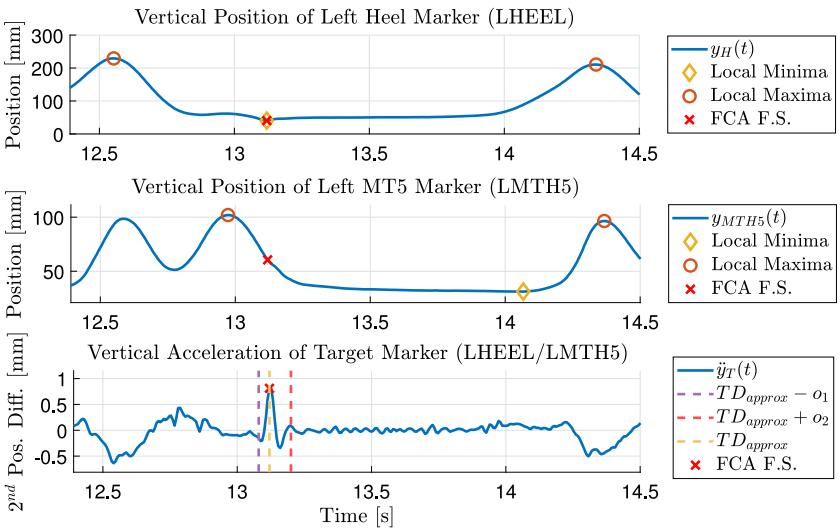

Fig. 2. Example of the foot-strike identification using the FCA. Top and middle subplots show the vertical position of the heel ($LHEEL$) and MTH5 ($LMTH5$) markers at a subject's left foot with respect to time, respectively. Bottom subplot depicts the vertical acceleration of the target marker ($LHEEL/LMTH5$) with respect to time. Diamonds ($\diamond$) and circles ($\circ$) indicate local minima and maxima of each signal in the corresponding subplot, respectively. Crosses ($\times$) illustrate foot-strike events identified using the FCA. Dashed lines represent the time instances defining the TI interval together with the TD_{approx} instance. Foot-strikes are defined as the most prominent local maxima in the vertical acceleration of the target marker during the time interval TI.

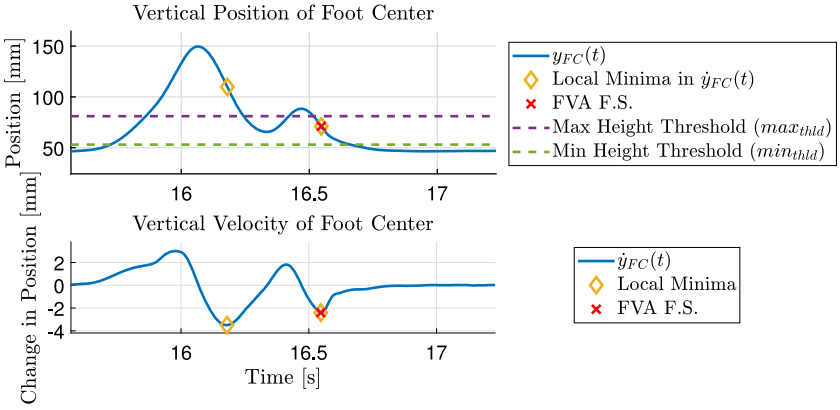

Fig. 3. Example of the foot-strike identification using the FVA. Top and bottom subplots show the vertical position and velocity of the foot center at a subject's left foot with respect to time, respectively. Diamonds ($\diamond$) indicate local minima in the vertical velocity of the foot center. Crosses ($\times$) illustrate foot-strike events identified using the FVA. Dashed lines represent the imposed constraints on the prominent local minima. Foot-strikes are defined as prominent negative local maxima in the foot center's vertical velocity, satisfying the imposed constraints.

information could be exploited to avoid false foot-strike estimations, hence improving the accuracy of the FPOSV. It should be noted that this feature is only observed during treadmill walking, hence the algorithm is not suitable for overground walking.

Initially in the implementation, the same real-time filtering conditions were applied, as in the previous algorithms. However, unlike the previous algorithms, a real-time implementation was designed for the F-VESPA.

For each incoming sample, the current vertical and sagittal velocities are calculated using a first-order finite difference approximation[3]:

$$dy_H(k) \triangleq \Delta y_H(k) = y_H(k) - y_H(k-1), \tag{2}$$

$$dx_H(k) \triangleq \Delta x_H(k) = x_H(k) - x_H(k-1), \tag{3}$$

where $y_H(k)$ and $x_H(k)$ are the filtered vertical and sagittal positions of the heel marker at the sample k, respectively, and $dy_H(k)$, $dx_H(k)$ are the corresponding velocities. Next, all future samples are ignored until a local maximum with a temporal prominence of two past and two future samples is found in the vertical velocity that exceeds a specific threshold (y_{GM}). This criterion is defined in the following equations:

$$dy_H(k) < 0 \; and \; dy_H(k-1) \leq 0, \tag{4}$$

$$dy_H(k-2) \geq 0 \; and \; dy_H(k-3) \geq 0, \tag{5}$$

$$y_H(k-2) > y_{GM}. \tag{6}$$

If all above conditions are met, the corresponding sample $(k-2)$ is defined as the "global" maximum k_{GM} for that gait cycle, and a search for local minima is initiated. Then, for each upcoming sample, the vertical velocity is computed again using Eq. (2), and all samples are ignored until a local minimum with a temporal prominence of three past and one future samples is found, i.e. meeting the conditions listed below:

$$dy_H(k) \geq 0, \tag{7}$$

$$dy_H(k-i) \leq 0 \; \forall \; i \in \{1,2,3\}. \tag{8}$$

system whether is going to be negative or positive. That said, the proposed algorithm is based on the fact that the sign is fixed.

[3] Since only the velocity's sign is of interest, the fixed temporal element dt is omitted.

Algorithm 1 F-VESPA

procedure F-VESPA (y^r_H = raw vertical position of heel marker, x^r_H = raw sagittal position of heel marker, f = boolean flag)
  $f = 0$ ▷ Disable search for local minima
  $y_{min} = 30\ mm$ ▷ Define fixed parameter
  while *true* **do** ▷ New motion capture sample
    Obtain $[k, y^r_H(k), x^r_H(k)]$ from motion capture system
    $[y_H(k), x_H(k)] \leftarrow$ Filter (y^r_H, x^r_H)
    Derive $dy_H(k)$ and $dx_H(k)$ ▷ Eqs. (2), (3)
    if $dy_H(k) < 0$ & $dy_H(k-1) \leq 0$ **then** ▷ Eq. (4)
      if $dy_H(k-2) \geq 0$ & $dy_H(k-3) \geq 0$ **then** ▷ Eq. (5)
        if $y_H(k-2) > y_{GM}$ **then** ▷ Eq. (6)
          $k_{GM} = k-2$ ▷ **"Global" maximum**
          $f = 1$ ▷ Initiate search for local minima
        end if
      end if
    end if
    if $f \neq 0$ & $dy_H(k) \geq 0$ **then** ▷ Eq. (7)
      if $dy_H(k-i) \leq 0\ \forall\ i \in \{1,2,3\}$ **then** ▷ Eq. (8)
        if $dx_H(k-1) < 0$ **then** ▷ Eq. (9)
          $k_{HS} = k-1$ ▷ **Foot-strike**
          $y_{GM} = y_{min} + y_H(k_{HS})$ ▷ Eq. (10)
          $f = 0$ ▷ Disable search for local minima
        end if
      end if
    end if
  end while
end procedure

Algorithm 1: The pseudo-code for the proposed F-VESPA algorithm.

When such a point is found, the corresponding sign of the sagittal velocity is checked. The point is kept only if the sign is negative, while discarded if positive, i.e. the condition to be met is:

$$dx_H(k-1) < 0. \tag{9}$$

If the condition is satisfied, then the sample $(k-1)$ is defined as the foot-strike event (k_{HS}) for that gait cycle. Based on the vertical position of the heel marker at foot-strike, the y_{GM} threshold is updated:

$$y_{GM} = y_{min} + y_H(k_{HS}), \tag{10}$$

where y_{min} is a fixed variable equal to 30 mm that represents a sufficient height distance between the vertical position of the heel at foot-strike and its next "global" maximum. Moreover, the search for local minima (foot-strikes) is disabled until the next "global" maximum is found and the same procedure is repeated until the end of the trial. The pseudo-code for the proposed F-VESPA algorithm is given in Algorithm 1. Fig. 4 demonstrates an example of foot-strike identification using the F-VESPA.

3. Results

In this section, the performance of the FCA (offline), FVA (offline) and F-VESPA (real-time) in identifying foot-strike events is evaluated. All algorithms were implemented and executed in MATLAB™ version 9.7 (R2019b) (The MathWorks, Natick, MA, USA). The ground truth of the foot-strike event times were determined using the force plate measurements as discussed in Section 2.1. The accuracy of each method is quantified by defining the estimation error in frames between the real (ground truth) and estimated timing of the foot-strike. In order for the comparison to be more generalizable, all the errors are reported in frames, or samples, without imposing a specific sampling frequency for the kinematic data.

The implemented algorithms were evaluated using nine young adults from the aforementioned dataset (Fukuchi et al., 2018b), who shared similar nominal speeds with statistical significance ($p < .001$, Cohen's d (effect size): $d = 24.41$, 95% Confidence Interval: $CI = (1.7659\ \text{to}\ 1.8807)$ m/s), across 8 different walking speeds around their nominal speed. Their average nominal speed was equal to $v_m = 1.26 \pm 0.05$ m/s.

3.1. Evaluation and comparison of F-VESPA to FCA, and FVA

In addition to the true and absolute errors of estimation, the true time delay required for the calculation of the foot-strike estimation was computed for each algorithm.

As discussed in Section 2.4, the F-VESPA was designed for real-time deployment. Therefore, real-time conditions were simulated for the evaluation of its performance. In detail, for a given trial, each sample was processed one by one, with the algorithm having no access to any future samples. As a consequence, in order to determine whether a given sample has a specific temporal prominence (i.e. Eqs. (4), (5), (8)), the algorithm had to first process the required number of future samples. This property introduces an inherent time delay that has to be accounted for when evaluating performance. The inherent delay of its predictions is equal to one sample for all cases, as it requires a maximum number of one future sample for the identification of foot-strike events using Eqs. (7), (8), (9).

In contrast, only offline implementations were possible for the FCA and the FVA. Specifically, in both algorithms the apriori knowledge of the whole trial was required, since they utilize local extrema with a specific prominence. For comparison purposes, only the time delays associated with temporal prominence and time windows are analyzed. For the FCA, knowledge over the whole time interval TI is required as shown in Eq. (1), which introduces a delay of 12 samples. Additionally, local minima required a minimum separation, which was optimized to maximize the performance of the algorithm. Therefore, the time delay for the FCA was defined as the sum of the two components. For the FVA, only the minimum separation for the local minima introduced additional time delay, which was again optimized to maximize the performance of the algorithm.

The results of the FCA, FVA and F-VESPA across all subjects and walking speeds are shown in Table 2. For each walking speed, the mean absolute error (MAE) and mean time delay (MTD) are shown, along with standard deviations. The MAE quantifies the accuracy of each algorithm in estimating foot-strike events without taking into account the aforementioned time delays. The MTD shows the error in estimating the foot-strike event due to the inherent delay of each algorithm. This is of high importance since we are interested in real-time foot-strike event detection and the MTD captures how late the predictions would be in real-time. The total mean absolute error of each algorithm for a specific speed is defined as the sum of the respective MAE and MTD components.

Amongst all implemented algorithms, the F-VESPA exhibits the lowest total error in frames across all speeds and subjects. Although FVA seems to have slightly better performance than the F-VESPA, if only MAE is considered across all speeds, its standard deviation is significantly larger than that of F-VESPA. Moreover, the MAE performance of the FVA declined as the treadmill speed increased, while the performance of the F-VESPA is not affected by walking speed. The error induced due to the inherent time delay of the F-VESPA is equal to one across all trials, hence no deviation is observed. In contrast, both the FCA and FVA have significantly high MTD values, both in terms of magnitude and deviation, bringing their total error higher than that of the F-VESPA across all speeds.

The statistical differences of accuracy (true error of estimation) between the algorithms were tested using paired t-tests. In both pairs (F-VESPA, FCA) and (F-VESPA, FVA) the null hypothesis was rejected, indicating statistically different distributions of errors among the algorithms. P-values, Cohen's d (effect sizes) and 95% Confidence Intervals (CI) are reported in Table 3. Significance level was set at $\alpha = 5\%$.

The distribution of true errors e_t across all trials was calculated for each algorithm without including the inherent time delays, and normal distribution fit was attempted. The histograms of the errors are shown in Fig. 5. The histogram data were tested for normal distribution using the Kolmogorov–Smirnov test (Massey Jr., 1951). In all three cases, the null hypothesis was rejected using the default significance

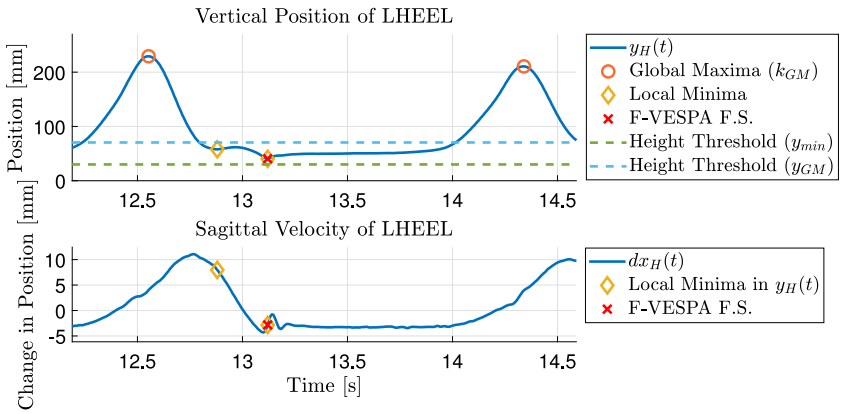

Fig. 4. Example of foot-strike identification using the F-VESPA. Top and bottom subplots show the vertical position and sagittal velocity of the heel marker at a subject's left foot with respect to time, respectively. Circles (∘) indicate "global" maxima and diamonds (⋄) indicate prominent local minima in the vertical position. Crosses (×) illustrate foot-strike events identified using the F-VESPA. Dashed lines represent the height thresholds applied. Foot-strikes are defined as prominent local minima in the vertical position $y_H(t)$ that correspond to a negative sagittal velocity $dx_H(t)$.

Table 2
Evaluation and comparison of the FCA, FVA and F-VESPA algorithms across all treadmill speeds for young subjects. MAE columns represent the mean absolute errors and standard deviations in frames of the FCA, FVA and F-VESPA algorithms, respectively. MTD columns represent the mean time delays and standard deviations in frames of the FCA, FVA and F-VESPA algorithms, respectively. For each speed, the MAE and MTD pair that resulted in the lowest total error is highlighted in bold. The total error of each algorithm for a specific treadmill speed is defined as the sum of the MAE and MTD values.

Treadmill speed (m/s)	FCA		FVA		F-VESPA	
	MAE (SD)	MTD (SD)	MAE (SD)	MTD (SD)	MAE (SD)	MTD (SD)
T01: 0.50	4.91 (0.43)	30.11 (17.52)	2.49 (0.96)	11.22 (8.41)	**4.36 (0.41)**	**1 (0)**
T02: 0.69	4.89 (0.34)	37.78 (11.29)	2.84 (0.79)	8.0 (6.46)	**4.27 (0.22)**	**1 (0)**
T03: 0.88	4.90 (0.14)	30.0 (10.71)	3.13 (0.87)	5.67 (5.61)	**4.29 (0.15)**	**1 (0)**
T04: 1.07	5.03 (0.04)	28.0 (8.89)	3.24 (0.84)	5.44 (5.27)	**4.30 (0.09)**	**1 (0)**
T05: 1.26	5.08 (0.16)	31.56 (19.63)	3.53 (0.90)	6.22 (3.93)	**4.27 (0.17)**	**1 (0)**
T06: 1.45	4.99 (0.19)	32.67 (16.87)	3.56 (0.85)	4.11 (5.01)	**4.26 (0.16)**	**1 (0)**
T07: 1.64	4.97 (0.12)	45.78 (25.79)	3.78 (0.90)	3.0 (4.58)	**4.22 (0.15)**	**1 (0)**
T08: 1.82	4.93 (0.15)	37.78 (23.05)	4.18 (0.76)	1.67 (3.32)	**4.20 (0.19)**	**1 (0)**

Table 3
Confidence intervals for the evaluation and comparison of the FCA, FVA and F-VESPA algorithms across all treadmill speeds for young subjects. For each algorithm, the 95% confidence intervals for both the absolute error and the time delay are reported. The total error of each algorithm for a specific treadmill speed is defined as the sum of the absolute error and the time delay values.

Treadmill speed (m/s)	FCA		FVA		F-VESPA	
	Absolute error	Time delay	Absolute error	Time delay	Absolute error	Time delay
T01: 0.50	4.58 to 5.24	16.65 to 43.58	1.75 to 3.23	4.76 to 17.60	4.05 to 4.68	1 to 1
T02: 0.69	4.62 to 5.15	29.10 to 46.46	2.23 to 3.45	3.03 to 12.97	4.10 to 4.44	1 to 1
T03: 0.88	4.79 to 5.0	21.77 to 38.23	2.46 to 3.80	1.35 to 9.98	4.17 to 4.40	1 to 1
T04: 1.07	5.0 to 5.06	21.17 to 34.83	2.60 to 3.89	1.39 to 9.50	4.23 to 4.37	1 to 1
T05: 1.26	4.96 to 5.21	16.46 to 46.65	2.84 to 4.21	3.20 to 9.24	4.15 to 4.40	1 to 1
T06: 1.45	4.85 to 5.14	19.70 to 45.63	2.91 to 4.21	0.26 to 7.96	4.14 to 4.38	1 to 1
T07: 1.64	4.88 to 5.06	25.95 to 65.60	3.09 to 4.47	−0.52 to 6.52	4.10 to 4.34	1 to 1
T08: 1.82	4.81 to 5.04	20.06 to 55.50	3.59 to 4.77	−0.88 to 4.22	4.06 to 4.35	1 to 1

threshold ($p < .001$). Therefore it was determined that the e_t data of all three algorithms do not originate from normal distributions. As a consequence, we choose to compare the data by median and range. Furthermore, the paired t-tests between the implemented algorithms were verified ($p < .001$) using the non-parametric alternative through the Kruskal–Wallis test (Kruskal and Wallis, 1952). Amongst all implemented algorithms, the F-VESPA exhibits the lowest median (4) and range (from 2 to 7) in frames across all trials. The median corresponds to a total error of 5 (4+1) frames or 33 ms (150 Hz sampling frequency). The FCA and the FVA have a larger and smaller median of 5 and 3 frames, respectively, while the FCA is more consistent as it has a range from 2 to 8 frames. On the other hand, the FVA has a significantly higher range from −2 to 10 frames.

4. Discussion

This work evaluated a new kinematic algorithm for the detection of the heel-strike event during gait in real-time. Although several kinematic algorithms have predicted foot-strike events with high accuracy in the past, such as the FCA (Maiwald et al., 2009), FVA (O'Connor et al., 2007) and FPOSV (Alton et al., 1998; Fellin et al., 2010), they have been implemented mostly offline (Fellin et al., 2010; Sinclair et al., 2011; Alvim et al., 2015), while their precision and latency have not been validated in real-time implementation (Roeles et al., 2018; Barkan et al., 2014). This is a major limitation that prevents the use of such algorithms in real-time. This work advances the field by proposing the F-VESPA, an extended version of FPOSV, which does not need access to future data points, and therefore can be implemented in real-time without loss of accuracy. The novel utilization of the sagittal position of the heel marker in the F-VESPA allows the

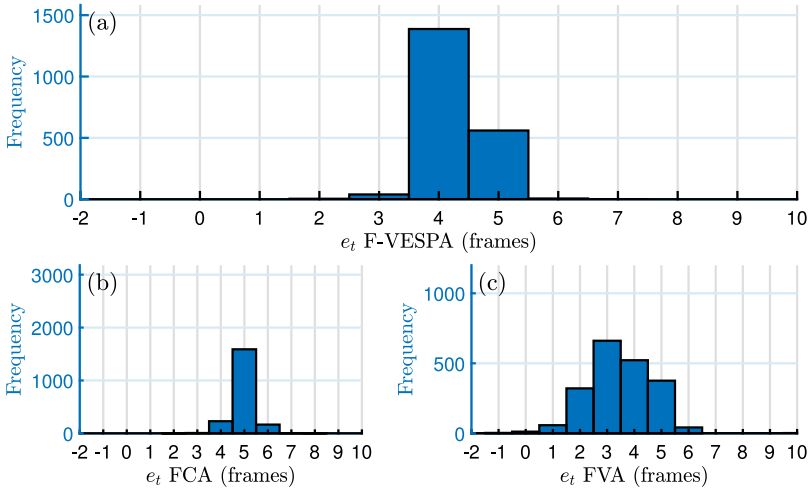

Fig. 5. Histograms of true error e_t for young subjects in frames for F-VESPA (a), FCA (b), and FVA (c). Bars represent the frequency of each true error value in gait cycles.

precise detection of foot-strikes, without depending on complex and computational intensive tools. Direct comparison between the FPOSV (real-time implementation) and the F-VESPA showed that the latter was more accurate across multiple subjects and walking speeds. The performance of the FPOSV was orders of magnitude worse, hence the respective analysis was omitted for brevity.

In addition to the real-time implementation, another feature that makes the F-VESPA unique is its overall efficiency, in terms of both accuracy and latency. That was shown in a comparison of the F-VESPA with two prominent existing algorithms: the FCA and the FVA. Real-time conditions were simulated for the execution of the F-VESPA, while the FCA and FVA were implemented in offline conditions, by having access to future data samples. Namely, the FCA and FVA required extensive parameter tuning to maximize performance, based on the knowledge of future data that would not be available in real-time conditions. Moreover, for comparison purposes, an ideal scenario for their latency was considered, as major time delay components were ignored. On the other hand, the F-VESPA had access only to the current and previous samples. All local extrema had to be found without utilizing any sophisticated functions, while the utilized parameters were not tuned to the given dataset. Furthermore, the true latency was considered, as it resulted from the algorithm's inherent time delay of one sample. As a result, the conditions of the comparison between the real-time F-VESPA and the offline FCA and FVA favored significantly the latter. Regardless, the F-VESPA managed to outperform the other two algorithms across all speeds and subjects, by exhibiting an average total error of 33 ms, as shown in Section 3.

Although the proposed algorithm achieved reduced latency and improved accuracy, it should be noted that the F-VESPA was tested only in normal gait. As this work is intended for rehabilitation purposes on impaired individuals, future work is underway to examine the performance of the algorithm on subjects with pathological gait. Furthermore, the F-VESPA is only suitable for treadmill walking, which mainly takes place in indoor environments. On the other hand, some potential fields of application, such as FES and wearable devices, provide practical benefits outside a motion laboratory. However, these fields require extensive time spent inside a lab for calibration and training phases, especially during the development of new technologies. As a consequence, motion capture could be utilized to stream kinematic data in real-time to the employed device. Therefore, the proposed algorithm could be implemented, hence providing reliable and robust gait segmentation in real-time.

In conclusion, this paper introduces a novel real-time kinematic algorithm for detecting foot-strike events during treadmill walking across different subjects and speeds. The algorithm was shown to have superior efficiency and robustness compared to previous works, even though they were implemented offline in much more favorable conditions than the proposed algorithm. As real-time detection of gait events is important for rehabilitation and gait analysis studies, this work can significantly advance the field by allowing robust and accurate detection of gait events in real-time using only kinematic data.

CRediT authorship contribution statement

Chrysostomos Karakasis: Conceptualization, Methodology, Software, Writing – original draft. **Panagiotis Artemiadis:** Writing – review & editing, Funding acquisition, Supervision.

Declaration of competing interest

The authors declare that they have no known competing financial interests or personal relationships that could have appeared to influence the work reported in this paper.

Acknowledgments

This material is based upon work supported by the National Science Foundation under Grants No. #2020009, #2015786, #2025797, and #2018905. This scientific paper was partially supported by the Onassis Foundation - Scholarship ID: F ZQ029-1/2020-2021.

All authors approved the final submitted draft.

References

Alton, F., Baldey, L., Caplan, S., Morrissey, M., 1998. A kinematic comparison of overground and treadmill walking. Clin. Biomech. 13 (6), 434–440.

Alvim, F., Cerqueira, L., Netto, A.D., Leite, G., Muniz, A., 2015. Comparison of five kinematic-based identification methods of foot contact events during treadmill walking and running at different speeds. J. Appl. Biomech. 31 (5), 383–388.

Barkan, A., Skidmore, J., Artemiadis, P., 2014. Variable stiffness treadmill (VST): A novel tool for the investigation of gait. In: 2014 IEEE International Conference on Robotics and Automation. (ICRA), IEEE, pp. 2838–2843.

Desailly, E., Daniel, Y., Sardain, P., Lacouture, P., 2009. Foot contact event detection using kinematic data in cerebral palsy children and normal adults gait. Gait Posture 29 (1), 76–80.

Dingwell, J., Cusumano, J.P., Cavanagh, P., Sternad, D., 2001. Local dynamic stability versus kinematic variability of continuous overground and treadmill walking. J. Biomech. Eng. 123 (1), 27–32.

Dollar, A.M., Herr, H., 2008. Design of a quasi-passive knee exoskeleton to assist running. In: 2008 IEEE/RSJ International Conference on Intelligent Robots and Systems. IEEE, pp. 747–754.

Drolet, M., Yumbla, E.Q., Hobbs, B., Artemiadis, P., 2020. On the effects of visual anticipation of floor compliance changes on human gait: Towards model-based robot-assisted rehabilitation. In: 2020 IEEE International Conference on Robotics and Automation. (ICRA), IEEE, pp. 9072–9078.

Fellin, R.E., Rose, W.C., Royer, T.D., Davis, I.S., 2010. Comparison of methods for kinematic identification of footstrike and toe-off during overground and treadmill running. J. Sci. Med. Sport 13 (6), 646–650.

[dataset], Fukuchi, C., Fukuchi, R., Duarte, M., 2018a. A public data set of overground and treadmill walking kinematics and kinetics of healthy individuals. Figshare Dataset http://dx.doi.org/10.6084/m9.figshare.5722711.v4.

Fukuchi, C.A., Fukuchi, R.K., Duarte, M., 2018b. A public dataset of overground and treadmill walking kinematics and kinetics in healthy individuals. PeerJ 6, e4640.

Hanlon, M., Anderson, R., 2009. Real-time gait event detection using wearable sensors. Gait Posture 30 (4), 523–527.

Holgate, M.A., Sugar, T.G., Bohler, A.W., 2009. A novel control algorithm for wearable robotics using phase plane invariants. In: 2009 IEEE International Conference on Robotics and Automation. IEEE, pp. 3845–3850.

Hreljac, A., Marshall, R.N., 2000. Algorithms to determine event timing during normal walking using kinematic data. J. Biomech. 33 (6), 783–786.

Hreljac, A., Stergiou, N., 2000. Phase determination during normal running using kinematic data. Med. Biol. Eng. Comput. 38 (5), 503–506.

Kadoya, S., Nagaya, N., Konyo, M., Tadokoro, S., 2014. A precise gait phase detection based on high-frequency vibration on lower limbs. In: 2014 IEEE International Conference on Robotics and Automation. (ICRA), IEEE, pp. 1852–1857.

Kang, I., Molinaro, D.D., Duggal, S., Chen, Y., Kunapuli, P., Young, A.J., 2021. Real-time gait phase estimation for robotic hip exoskeleton control during multimodal locomotion. IEEE Robot. Autom. Lett. 6 (2), 3491–3497.

Karakasis, C., Artemiadis, P., 2021. F-VESPA: A kinematic-based algorithm for real-time heel-strike detection during walking. In: 2021 IEEE/RSJ International Conference on Intelligent Robots and Systems. (IROS), IEEE, (in press).

Kormushev, P., Ugurlu, B., Colasanto, L., Tsagarakis, N.G., Caldwell, D.G., 2012. The anatomy of a fall: Automated real-time analysis of raw force sensor data from bipedal walking robots and humans. In: 2012 IEEE/RSJ International Conference on Intelligent Robots and Systems. IEEE, pp. 3706–3713.

Kruskal, W.H., Wallis, W.A., 1952. Use of ranks in one-criterion variance analysis. J. Amer. Statist. Assoc. 47 (260), 583–621.

Leitch, J., Stebbins, J., Paolini, G., Zavatsky, A.B., 2011. Identifying gait events without a force plate during running: A comparison of methods. Gait Posture 33 (1), 130–132.

Lim, B., Kim, K., Lee, J., Jang, J., Shim, Y., 2015. An event-driven control to achieve adaptive walking assist with gait primitives. In: 2015 IEEE/RSJ International Conference on Intelligent Robots and Systems. (IROS), IEEE, pp. 5870–5875.

Lind, R.F., Love, L.J., Rowe, J.C., Pin, F.G., 2009. Multi-axis foot reaction force/torque sensor for biomedical applications. In: 2009 IEEE/RSJ International Conference on Intelligent Robots and Systems. IEEE, pp. 2575–2579.

Maiwald, C., Sterzing, T., Mayer, T., Milani, T., 2009. Detecting foot-to-ground contact from kinematic data in running. Footwear Sci. 1 (2), 111–118.

Massey Jr., F.J., 1951. The Kolmogorov-Smirnov test for goodness of fit. J. Amer. Statist. Assoc. 46 (253), 68–78.

Mickelborough, J., Van Der Linden, M., Richards, J., Ennos, A., 2000. Validity and reliability of a kinematic protocol for determining foot contact events. Gait Posture 11 (1), 32–37.

O'Connor, C.M., Thorpe, S.K., O'Malley, M.J., Vaughan, C.L., 2007. Automatic detection of gait events using kinematic data. Gait Posture 25 (3), 469–474.

Pappas, I.P., Popovic, M.R., Keller, T., Dietz, V., Morari, M., 2001. A reliable gait phase detection system. IEEE Trans. Neural Syst. Rehabil. Eng. 9 (2), 113–125.

Perry, J., Davids, J.R., et al., 1992. Gait analysis: normal and pathological function. J. Pediatric Orthopaedics 12 (6), 815.

Roeles, S., Rowe, P., Bruijn, S., Childs, C., Tarfali, G., Steenbrink, F., Pijnappels, M., 2018. Gait stability in response to platform, belt, and sensory perturbations in young and older adults. Med. Biol. Eng. Comput. 56 (12), 2325–2335.

Rueterbories, J., Spaich, E.G., Larsen, B., Andersen, O.K., 2010. Methods for gait event detection and analysis in ambulatory systems. Med. Eng. Phys. 32 (6), 545–552.

Saccares, L., Sarakoglou, I., Tsagarakis, N.G., 2018. A novel joint torque estimation method and sensory system for assistive lower limb exoskeletons. In: 2018 IEEE/RSJ International Conference on Intelligent Robots and Systems. (IROS), IEEE, pp. 1–9.

Schache, A.G., Blanch, P.D., Rath, D.A., Wrigley, T.V., Starr, R., Bennell, K.L., 2001. A comparison of overground and treadmill running for measuring the three-dimensional kinematics of the lumbo–pelvic–hip complex. Clin. Biomech. 16 (8), 667–680.

Sinclair, J.K., Edmundson, C.J., Brooks, D., Hobbs, S.J., 2011. Evaluation of kinematic methods of identifying gait events during running. Int. J. Sports Sci. Eng. 5 (3), 188–192.

Sinclair, J., Hobbs, S.J., Protheroe, L., Edmundson, C.J., Greenhalgh, A., 2013. Determination of gait events using an externally mounted shank accelerometer. J. Appl. Biomech. 29 (1), 118–122.

Taborri, J., Palermo, E., Rossi, S., Cappa, P., 2016. Gait partitioning methods: A systematic review. Sensors 16 (1), 66.

Tao, W., Liu, T., Zheng, R., Feng, H., 2012. Gait analysis using wearable sensors. Sensors 12 (2), 2255–2283.

Walsh, C.J., Pasch, K., Herr, H., 2006. An autonomous, underactuated exoskeleton for load-carrying augmentation. In: 2006 IEEE/RSJ International Conference on Intelligent Robots and Systems. IEEE, pp. 1410–1415.

Zeni Jr., J., Richards, J., Higginson, J., 2008. Two simple methods for determining gait events during treadmill and overground walking using kinematic data. Gait Posture 27 (4), 710–714.